

DEVELOPMENT OF GEOHYDROLOGIC MODEL OF THE WILDCAT FAULT ZONE

Kenzi Karasaki¹, Christine Doughty¹, and Junichi Goto²

¹Lawrence Berkeley National Laboratory
Berkeley, California, 94720, USA
e-mail: kkarasaki@lbl.gov, CADoughty@lbl.gov

²Nuclear Waste Management Organization of Japan
Tokyo, Japan
e-mail: jgoto.numo.or.jp

ABSTRACT

We have conducted field investigations of the Wildcat Fault starting with a literature survey, an aero-photo-based geomorphological study, geologic mapping, geophysical surveys, trenching, and borehole drilling and hydraulic testing in the LBNL area. A geologic model was constructed, which became the basis of the hydrologic model. Here, we outline the effort of constructing the geohydrologic model of Strawberry Canyon, the area on which our study focuses. We also created an East Canyon submodel, which is part of Strawberry Canyon.

The models were constructed by using PetraSim commercial software, which is a pre- and post-processor for TOUGH2. One of our goals is to understand the role of the Wildcat Fault in controlling the natural-state groundwater flow. With limited data in numbers and areal extent, we hope to build a model that is valid for a scale larger than the observation area. We performed both manual and automated inversion analysis and produced reasonable matches between the observed head data and model predictions. By varying the structure of the Wildcat Fault, we found that the base-case representation, which includes a high-permeability damage zone and a low-permeability fault core, best matches the observed head data. Using the submodel, we conducted a two-phase nonisothermal simulation utilizing the pressure and temperature data from the boreholes. We also used the information obtained from pump tests, including permeability anisotropy of the fault plane.

After parameter searches, we were able to match the head and temperature profiles along boreholes relatively well. We then used the best

matching models to predict the rate of head decline during a dry period, and found that an anisotropic fault zone with 5% porosity predicts the rate of decline reasonably well. There is the potential that the rate of decline may be useful in estimating the permeability downstream, where there are no boreholes for observation/testing.

INTRODUCTION

The primary objective of the Fault Zone Hydrology Project is to develop an effective and reliable methodology for fault-zone characterization. To this end, we have conducted field investigations of the Wildcat Fault (WF) starting with a literature survey, an aero-photo-based geomorphological study, geologic mapping, geophysical surveys, trenching, borehole drilling, and hydraulic testing in the LBNL area. According to the systematized investigation flow proposed in Karasaki et al. (2009, 2010) and Kiho et al. (2012), a geologic model would be constructed as information and data gathered by the field investigation started to come in. Then, the geologic model would become the basis of a hydrologic model that honors hydraulic data obtained by passive and active hydrologic tests. The hydrologic model would then be used to make predictions of the outcome of the next stage of investigations, and to identify data holes (if any). Thus, the field investigation, geologic model, and hydrologic model would compose a circular feedback loop.

In the present paper, we outline the effort of constructing the geohydrologic model of the Strawberry Canyon (Berkeley, California), the basin within which our current study area is concentrated. We also created a smaller subregion model of the East Canyon. One of our

goals is to understand the role of the Wildcat Fault in controlling natural-state groundwater flow, and one means to assist in developing this understanding is to develop a numerical model of groundwater flow in the basin containing the fault. Our flow-modeling strategy was to calculate the natural-state flow field and also to investigate the transient inter-well response to drilling, well tests, long-term pumping, and seasonal fluctuations.

DATA AVAILABLE

A great deal of site characterization data is available from which to construct the model, including:

- Geologic map (Graymer, 2000; Karasaki et al., 2009, 2010, 2011; Kiho et al., 2012)
- Digital elevation model (up to 3 m resolution)
- Surface fault location in trenches (TR-1~5)
- Three vertical wells with geophysical log information and permanent pressure and temperature sensors at 5 depths (WF-1–WF-3)
- Two diagonal wells crossing the fault (WF-4 and WF-5)
- Two deep wells with water-level and pumping rate data (SSL-1 and 2)
- Flow rates for three existing wells/hydraugers (Lennert, BG-1, Quarry)
- Many shallow wells with water-level data and permeability estimates (often from slug tests) from the Site Environmental Remediation Project
- Precipitation record
- Air temperature record.

NUMERICAL SIMULATOR

The TOUGH2 code, a general purpose numerical simulator for fluid flow and heat transport in geological media (Pruess et al., 1999), is used for the numerical simulations. TOUGH2 preliminary simulations use the equation of state module EOS9, which considers single-phase liquid water or a unsaturated system in which the air is a passive spectator (a common soil-physics approximation) and temperature does

not change. Results of TOUGH2/EOS9 simulations include steady-state and transient hydraulic head distributions, infiltration rates, and flow rates from various outlets in the model (creeks, springs, hydraugers). We also use equation-of-state module EOS3 (which is non-isothermal and includes an active gas phase), for the East Canyon submodel. Temperature profiles in boreholes can provide up-flow or down-flow signatures of groundwater.

MODEL DOMAIN

Figure 1 shows a 3 m resolution digital elevation map (DEM) of the Berkeley Hills area. The map is shaded to show the topographic relief, so that basins are easily identified. Note that our study area is in a well-defined basin, Strawberry Canyon. We chose the model area to coincide with the basin, which covers the Strawberry Creek watershed east of the Hayward Fault. The model is roughly diamond-shaped, with diagonal lengths 3 km in the E-W direction and 2.4 km in the N-S direction. Boundaries to the northwest, northeast, and southeast were determined by following ridgelines on the DEM.

The surface trace of the Hayward Fault forms the southwest boundary of the model. It follows a strong break in slope between the hilly terrain of the model and the much gentler slope that extends to San Francisco Bay. The elevation along this boundary is gently undulating, with several creeks running NE-SW crossing the fault. The rectangular area is the University of California, Berkeley Campus. Note that there are several creeks running EW, which are the continuation of Strawberry Creek displaced by the Hayward Fault.

In the vertical direction, the model extends from the ground surface, which ranges from about 120 masl to 540 masl, to an elevation of -400 masl. No wells extend any deeper than 0 masl, but the large vertical extent is provided so that the model horizontal-to-vertical aspect ratio is near one, in order to not artificially constrain natural groundwater flow lines.

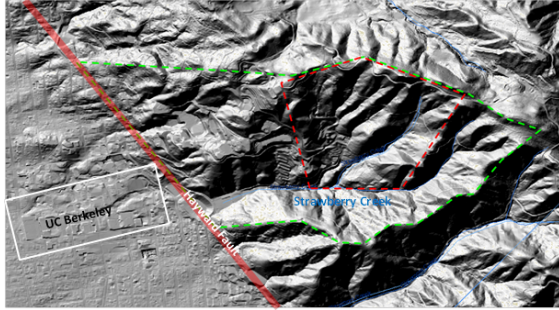


Figure 1. Shaded DEM map of the Berkeley Hills. The Strawberry Canyon model area is outlined in green. The red dashed line is the East Canyon Submodel area.

GEOLOGIC MODEL

The current geologic model used in the hydrologic simulation can be seen in Figure 2, based on available geologic maps and core analysis from five boreholes, WF-1 through WF-5. (Graymer, 2000; Karasaki et al., 2009, 2010, 2011, 2012; Kiho et al., 2012).

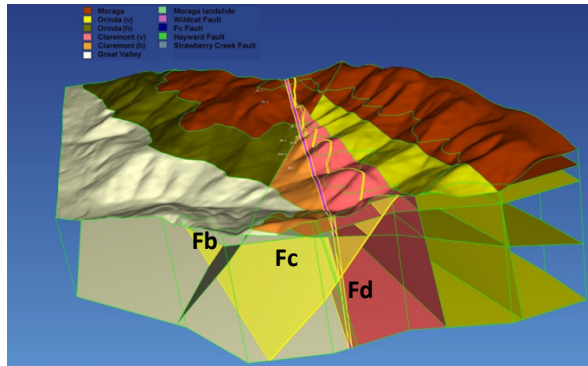


Figure 2. Perspective view of the geologic model showing faults and contacts between formations. Three faults are highlighted: the vertical Wildcat Fault (Fd), the sloping Fc and Fb structure.

Our geologic model essentially incorporates the Fb, Fc, and Fd structures proposed by Kiho et al. (2012), except our model assumes that Kiho et al.'s Fd-branch is the main Wildcat Fault. Fb is modeled as the geologic boundary between the Orinda Formation/San Pablo Group and Claremont Formation, without any thickness or independent permeability. Fc is modeled as a permeable structure, while Fd is modeled as a dual structure, with low permeability

perpendicular to the fault and high permeability parallel to the fault. All the features are treated as a plane. We assume that hydrologically there are two types of Orinda Formation and Claremont Formation. The Orinda Formation observed in WF-2, WF-3, and WF-4 appears to be subhorizontal, whereas the same formation on the east of the Wildcat Fault is reported to be subvertical, as is the Claremont Formation on the east side of the Wildcat Fault (Geomatrix, 2008). In general, a sedimentary layer is anisotropic, with a lower vertical permeability than horizontal when it is in the original depositional state. Therefore, we expect a lower permeability in the vertical direction of the Orinda Formation in the west, and vice versa on the east of the fault. As for the Claremont Formation, we assumed that the Claremont on the west is of a different material than on the east of the fault.

GRID

Strawberry Canyon Model

The preliminary numerical grid is constructed of 23 layers, each with the same lateral discretization. Lateral discretization is done with Voronoi tessellation and is variable, with finest resolution near the wells and Wildcat Fault, and a gradually coarsening grid beyond that (Figure 3). Each layer has 4295 gridblocks, and the total number of active gridblocks for the model is 101,024 (the top layer, representing the constant atmospheric boundary, is inactive).

Three features present in the numerical model are not shown in the original geologic model: the Hayward Fault, the Strawberry Creek Fault, and the Moraga landslide. The top of the model is defined by the DEM, and layer thickness gradually adjusts to conform to it. The top three layers are thinner, to better represent surface changes in topography. Permeabilities for all the materials are given in Table 1.

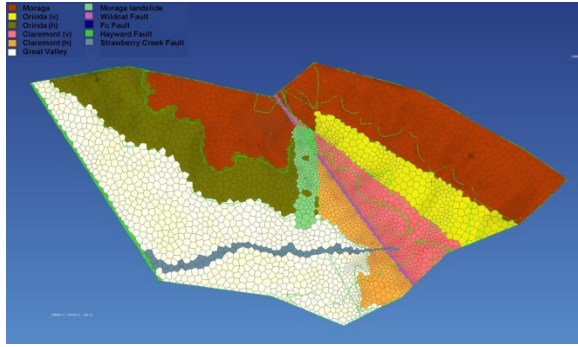


Figure 3. Plan view of the computational grid. Area around boreholes and along the Wildcat Fault is highly discretized.

Table 1. Permeability values used for the Strawberry Canyon model.

	Orinda		Claremont		Moraga	Great Valley	Fault Core	Fault Damage
	ToH	ToV	TcH	TcV				
Kx	8×10^{-16}	4×10^{-16}						
Ky	8×10^{-16}	4×10^{-16}	1×10^{-14}	1×10^{-15}	7×10^{-15}	7×10^{-15}	2.6×10^{-16}	1.3×10^{-13}
Kz	1×10^{-16}	8×10^{-16}						

East Canyon Sub-Model

The Strawberry Canyon model we have discussed above is based on a topography that clearly defines a closed basin, as shown in Figure 1. Using the hydraulic test results and pressure monitoring data, we estimated the permeability structure of the fault and the surrounding rocks. However, the parameters we obtained are, strictly speaking, only valid within the extent of the tests. We did find that long-term monitoring of seasonal changes in pressure may be useful in estimating the parameters of a larger volume outside of the well field. In particular, we found that the rate of decline in pressure during a dry season may be used to further calibrate or to verify the model. We used a Voronoi tessellation for the Strawberry Canyon model to keep the number of elements to a manageable size and still have fine discretization near a borehole. However, for the purpose of matching the static pressure and temperature profiles in boreholes and seasonal fluctuations due to rainfalls, no discretization is necessary in the vicinity of boreholes. Rather, a uniform grid with the finest affordable resolution is better for accuracy and manageability. For these reasons, we created a submodel, which we call the East Canyon Submodel, with regular

discretization, whose boundary is shown with the red broken line in Figure 1. As can be seen from the figure, the submodel captures a smaller but less well-defined basin. Figure 4 shows the numerical mesh of the East Canyon submodel. Table 2 shows the permeability values for the model.

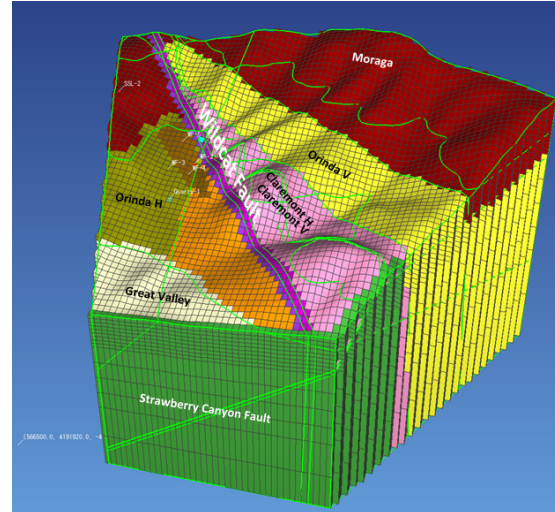


Figure 4. The numerical mesh of the east Canyon submodel. The Wildcat is modeled by two planes of low (purple) and high permeability (dark pink). The brown colored cells are the landslide material.

Table 2. Permeability values used for the East Canyon submodel. The anisotropic values for the fault reflect the pumping test results. The rest of the values are optimized values to match the observation data.

	Orinda		Claremont		Moraga	Great Valley	Landslide Material	Surface deposits	Fc	Fault Core	Fault Damage
	ToH	ToV	TcH	TcV							
Kx	1e-17	1E-17	1e-16	5e-17				2e-11		1e-17	1e-13
Ky	1e-17	1e-17	1e-16	5e-17	3e-15	1.5e-16	5e-16	2e-11	1e-13	1e-17	1e-13
Kz	1e-17	1e-17	5e-17	1e-16				5e-12		5e-18	1e-14

In the Strawberry Canyon model, we represented the duality of the Wildcat, i.e., high permeability along the fault and low permeability across it, by using a customized anisotropic permeability assignment. This is done by assigning high permeability between the cells of the same material but low permeability between different materials, specifically between the fault material and Orinda or Claremont Formations. In the East Canyon model, we represented the Wildcat with two side-by-side planar features—one represent-

ing the high permeability damaged zone and the other the low permeability core, as can be seen in Figure 4. We assigned a 10-to-1 ratio of anisotropy to the fault damage zone, based on interference tests. The recharge rate was determined by calibrating to the observed head data. The temperature profile data from WF boreholes indicate that the geothermal gradient is $\sim 4^{\circ}\text{C}/100\text{ m}$, which is relatively high. This is the result of the balance between cold rain recharging from the surface and the heat flux from the deeper subsurface. The bottom heat flux boundary condition was set at a constant rate of $85\text{ mW}/\text{m}^2$. Karasaki et al. (2011b) followed a similar approach by utilizing the temperature profile from boreholes to reduce the uncertainties of a geohydrologic model.

Simulation Results for Strawberry Canyon Model

Figure 5 compares hydraulic head values observed at the WF and SSL wells with model values for the simulation, with the best match between the two. The impact of the Wildcat Fault is apparent as a small jump in pressure. Several simulations were run with varying amounts of infiltration, including 50%–100% of the average annual precipitation rate of $1,000\text{ mm}/\text{yr}$. Here, infiltration is specified as 67% of precipitation. If precipitation is too low, well SSL-1 cannot sustain the observed pumping rate. Although the modeled heads are somewhat large for all the wells, the field-observed separation between wells WF-1 and WF-2 is captured by the model.

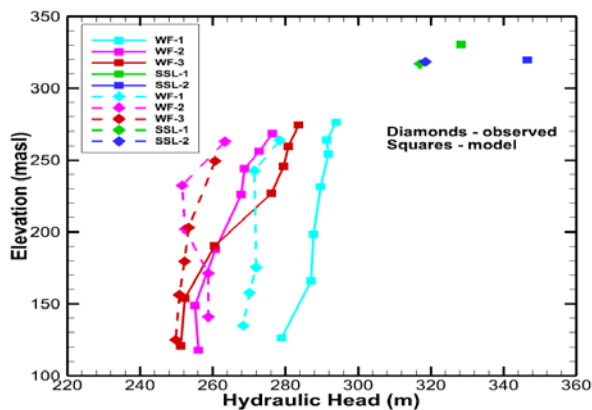


Figure 5. Comparison of modeled and observed hydraulic head measurements of the best case.

Simulation Results for East Canyon Sub-Model

Figure 6 shows the comparison between the observed head data in WF-1–WF-3 boreholes to one of the best simulation results. Note that the simulation reproduces the decreasing head distribution along the depth of the boreholes, the separation of heads between WF-1 and WF-2, and the low head anomaly in WF-2, which is likely caused by the permeable Fc feature that drains water to lower elevation. Figure 7 shows the simulated and observed temperature distributions along the WF boreholes. The solid and broken lines denote the observed and simulation results, respectively. As can be seen from the figure, the simulation reproduces the temperature profiles relatively well. The observed head data are represented by vertical line segments and the temperature data are continuous lines, because the head within an observation interval is assumed constant along the entire length as it is packed with coarse sand—whereas the temperature is thought to be linearly varying within an interval.

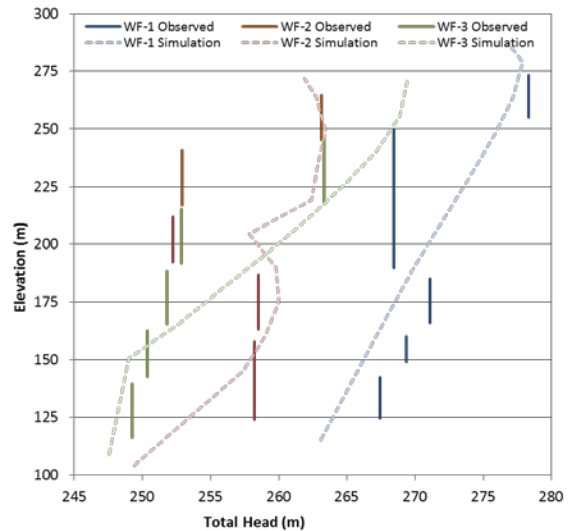


Figure 6. Comparison of simulation results with the observed head data of WF-1–WF-3. Note that the model reproduces the decreasing head with depth very well, as well as the low head anomaly in WF-1 possibly caused by the Fc fault.

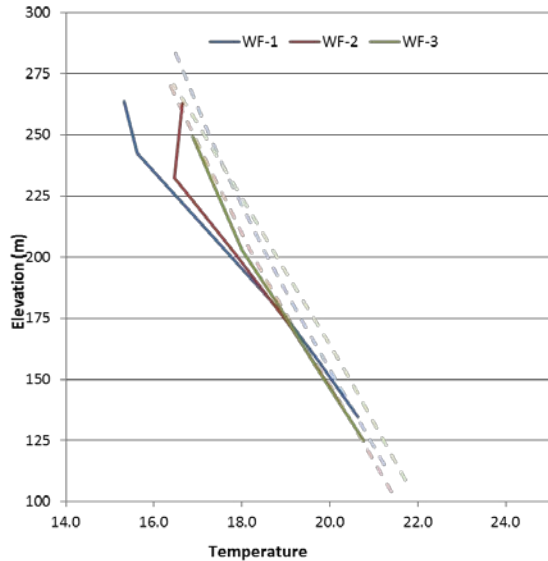


Figure 7. Comparison of simulation results with the observed temperature data of WF-1–WF-3. Note that the model reproduces the increasing temperature with depth very well below elevations of about 200 m.

This raises the question of the soundness of the traditional approach, in which observation intervals are very long and isolated by short packers. (In our case, grout was used in place of packers.)

Model Verification

Now we have an East Canyon submodel that reasonably reproduces the key aspects of head and temperature distribution observed in WF holes. In fact, several combinations of permeability produce similar goodness of fit. The next question is, how good are these models in predicting phenomena that were not used in the model calibration. The rate of head decline in WF-1 is ~ 2 m per half year during a dry period. We now try to see if the models predict a similar rate of decline by imposing a boundary condition simulating a wet and dry season. In developing the East Canyon model, we imposed a constant mass-flow-rate boundary condition (2.2×10^{-6} kg/m²s, equivalent to 7% of the annual average rainfall) on the surface and ran the simulation until steady state was reached, which is typically over 100,000 years of simulation time. We then use the steady-state condition produced by models that match the borehole head profiles as the initial condition to simulate rainfall during a rainy season, followed by a dry

season, for one year. Although we could use the actual daily rainfall data from the previous year as the boundary condition, we simplified the recharge event to a constant flux at 1×10^{-5} kg/m²s for 80 days for the rainy period and zero rainfall thereafter for one year.

Figure 8 shows the head transients at WF-1#3 from January 2011 through the end of February 2012, compared to the simulation results. The negative spikes in the observed data are due to pumping tests, which were not simulated. Both red and green lines have the same permeability structure that produces the match shown in Figure 6 and Figure 7. Specifically, they have a 10:1 anisotropy ratio in the fault zone. The only difference between the two curves is the porosity: the red line represents the case in which the fault zone rock has 10% porosity and the green, 5%. As can be expected, the larger porosity value shows a smaller head increase during the rainy period and slower head decrease during the dry period. Also shown is a modeled case with 10% porosity and an isotropic Fd feature (the pink curve), which matched the head profiles just as well as the previous two cases, but did not match the interference-test data as well. During the dry period from June and thereafter, the green curve declines in parallel with that of the observed data. The red line declines too slowly, while the pink declines too fast.

It is possible that having a constant recharge for 80 days represent the rainy period is too much of a simplification. The rate of decline during the dry period is controlled by the overall through-flow permeability from the area around the boreholes and to the discharge location, as well as by the porosity. Out of the three models, the 5% porosity model with 10:1 anisotropy ratio is the best model thus far. Note that porosity was not directly used in the calibration when we tried to match the head profiles along WF boreholes, since steady-state flow fields do not depend on porosity. Consequently, choosing the 5% porosity over 10% is actually a secondary calibration. It should be noted that a crude porosity estimate of 1.5% in the Moraga Formation, based on the level observation in SSL-1, is not reflected in the model. Although both numbers are at least in the ballpark, and the porosity variation in the Moraga Formation is expected to have little

impact on the borehole area because it is rather far away, the model run with the 1.5% porosity should be examined.

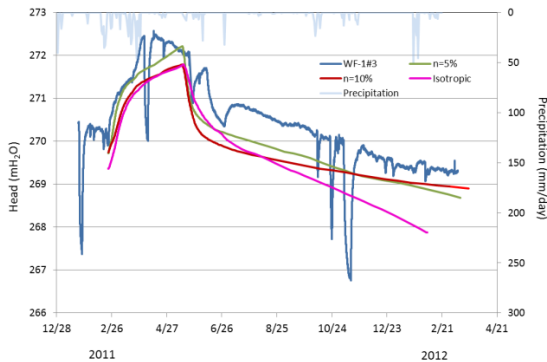


Figure 8. Comparison of simulation and observed head transients at WF-1#3 (blue) in response to seasonal rainfall using the best East Canyon submodel with 10% (red) and 5% (green) porosity, and isotropic Fd zone. The daily precipitation (light blue) is plotted against the right axis. Negative spikes in head in data are caused by pump tests, which were not modeled. Note that the head decline rate during the dry period is reproduced better assuming 5% average porosity.

CONCLUSIONS

We developed hydrogeologic models of the Wildcat Fault Zone that incorporates most of the geologic features at two different scales: the Strawberry Canyon basin model and the East Canyon submodel. We performed both manual and automated inversion analysis and produced reasonable matches between the observed head data and model predictions. We varied the infiltration rate and found that specifying infiltration as 67% of precipitation produced the best match to observed head data. This 67% rate is rather high and could possibly be an artifact of the way we handled recharge; actual recharge into the model may be much less. By varying the structure of the WF, we find that the representation that includes a high-permeability damage zone and a low-permeability fault core best matches the observed head data. It is possible to obtain better matches to the observed heads with a mesh refinement and local adjustments of parameter values. However, our objective here is to develop a methodology by which to understand the role of faults at a bigger scale through numerical modeling. If a better match is

obtained by local refinements, it is probably not very important at a larger scale, unless the refinement itself is some culmination of a larger scale property.

We constructed a submodel with uniform horizontal gridding and carried out a two-phase non-isothermal simulation utilizing the steady-state pressure and temperature data from the boreholes. For this submodel, we found that a recharge rate of 7% of the annual rainfall produces a best match, which is somewhat contradictory to the finding using the larger Strawberry Canyon model. Future studies will be directed at determining the source of this discrepancy.

We also obtained information by calibrating the model to interference well tests, such as the anisotropic permeability in the fault zone. After parameter searches, we were able to match the static head and temperature profiles along boreholes relatively well. We then used the best matching models to predict the rate of head decline during a dry period, and found that an anisotropic fault zone with 5% porosity predicts the rate of decline reasonably well. Further optimization may be possible by using more realistic boundary conditions. Thus, we used static and dynamic data to calibrate the submodel.

In theory, the larger the degree of freedom in the model, the easier it is to match the observed data. However, the goal here is not to simply match the observed data. Typically, data are limited in numbers and areal extent. We would like to build a model that is valid for a scale larger than the observation area. There is the potential that the rate of decline may be used to estimate the permeability downstream of the borehole complex, although more study is necessary to verify this claim.

It should be noted that because of the sloping nature of the model layers the gridding used in the model, in a strict sense, violates the conditions for the finite difference model approximation, where the line that connects adjacent element centers should be perpendicular to the element boundary. Although we don't expect a significant error, it should be examined.

REFERENCES

- Geomatrix, Preliminary Geologic Section Along Proposed Fourth Bore Alignment, Caldecott Tunnel Improvement Project, Alameda and Contra Costa Counties, California, 2008.
- Graymer, R.W., 2000, Geologic map and map database of the Oakland metropolitan area, Alameda, Contra Costa and San Francisco Counties, California. USGS Miscellaneous Field Studies MF3242g Version 1.0.
- Karasaki, K., Onishi, C.T., Doughty, C., Gasperikova, E., Peterson, P., Conrad, M., and Cook, P., 2011, Development of Hydrologic Characterization on Technology of Fault Zones – Phase II 2nd Report–, NUMO-LBNL-CRIEPI Collaboration Research Project.
- Karasaki, K., Onishi, C.T. and Zimmer, V., 2010, Development of Hydrologic Characterization on Technology of Fault Zones – Phase II Interim Report-, NUMO-LBNL-CRIEPI Collaboration Research Project.
- Karasaki, K., C.T. Onishi, and Y.S. Wu, 2009, Development of Characterization Technology for Fault Zones, LBNL-1635E, pp 157.
- Karasaki, K., K. Ito, Y.S. Wu, M. Shimo, A. Sawada, K. Maekawa, K. Hatanaka, 2011b, Uncertainty reduction of hydrologic models using data from surface-based investigation, doi: 10.1016/j.jhydrol.2011.03.039, Journal of Hydrology, 403 (1-2), pp49-57.
- Kiho, K., Ueta, K., Miyakawa, T., Hasegawa, T., Ito, H., Hamada, M., Nakada, H., Tanaka, S., and Tsukuda, K, 2012, CRIEPI Technical Report, Survey and Analysis related to Development of Hydrologic Characterization Technology of Fault Zones IV.
- Pruess, K., Oldenburg, C., and Moridis, G., TOUGH2 User's Guide, Version 2.0, Rep. LBNL-43134, Lawrence Berkeley National Laboratory, Berkeley, CA, 1999.